OPEN

MRI of the Central Lymphatic System: Indications, Imaging Technique, and Pre-Procedural Planning

Vishwan Pamarthi, MD, Waleska M. Pabon-Ramos, MD, MPH, Vincent Marnell, RT,(R)(CT),(MRI), and Lynne M. Hurwitz, MD

Abstract: Magnetic resonance imaging is increasingly being used to evaluate the lymphatic system. Advances in magnetic resonance (MR) software and hardware allow improved visualization of lymph nodes and lymphatic vessels. We describe how MR lymphangiography can be used to diagnose central lymphatic system anatomy and pathology, which can be used for diagnostic purposes or for pre-procedural planning.

Key Words: central lymphatic system, chylothorax, lymphatic malformations, MR lymphangiography, plastic bronchitis

(*Top Magn Reson Imaging* 2017;26:175–180)

The use of magnetic resonance imaging (MRI) to evaluate the central lymphatic system has been increasing as an alternative to traditional invasive lymphangiography. Recent advances in magnetic resonance (MR) software and hardware have allowed for improved visualization of the of lymphatic system on MR and increasing options for less invasive management of disorders of the lymphatic system.[1] In contrast to computed tomography and ultrasonography, which are used primarily to evaluate lymph nodes, MRI can be used to assess lymph nodes, the central and peripheral lymphatics. Imaging of the lymphatic system by MRI, previously referred to in the literature as MR lymphangiography (MRL), can be performed for diagnostic purposes or for pre-procedural planning. MRL can be performed with or without contrast administration into the lymphatic system, and can be used to assess the cisterna chyli, thoracic duct, and lymphatic disorders involving the mediastinum or chest wall. We herein describe indications, image acquisition protocols, image post-processing, and image interpretation for MRL.

ANATOMY OF THE CENTRAL LYMPHATIC SYSTEM

The central lymphatic system is composed of the cisterna chyli in the upper abdomen and the thoracic duct in the thorax. Lower extremity and retroperitoneal lymphatics converge with intra-abdominal lymphatics (hepatic, mesenteric, etc.) at the cisterna chyli, which is most frequently located in the retroperitoneum just anterior to the T12-L1 vertebral bodies in a right paramedian location. The cisterna chyli ranges from 0.5 to 2 cm in diameter. The thoracic duct extends cranially from the cisterna chyli and courses cephalad along the posterior mediastinum in a left paramedian location immediately anterior to the thoracic vertebral bodies. The thoracic duct receives multiple lymphatic branches that provide drainage to the lungs bilaterally. The cervical portion of the thoracic duct gradually courses anteriorly and to the left, connecting to the left central veins. The thoracic duct is most commonly a 2 to 4 mm diameter single vessel (Fig. 1).

Central lymphatic anatomy is frequently variable. While the most common location for the cisterna chyli is to the right of the aorta, a median or left paramedian location can also present as a normal variant. Approximately 30% of patients lack a cisterna chyli. These patients may have prominent retroperitoneal lymphatic vessels (Fig. 2). The thoracic duct may be variable in course: it may bifurcate or trifurcate anywhere along its course, including at the cervical portion before connecting to the central veins such that there are multiple outflow points into the central venous system. The thoracic duct may course in the posterior mediastinum, but in a right paramedian location with drainage into the right-sided central veins. Right-sided drainage has been reported in 2% to 3% of patients, and bilateral drainage in 1% to 1.5% of patients. The thoracic duct can have variable sites of drainage into central veins: internal jugular vein (60%), subclavian vein (15%), between the external and internal jugular veins (7%), between the external jugular and subclavian veins (2.5%), and the brachiocephalic vein (1.5%).[2,3]

MRL INDICATIONS

Lymphoceles

Pathophysiology

Lymphoceles are benign lesions that develop post-traumatically, most commonly from iatrogenic surgical injuries. Because they tend to be asymptomatic, many lymphoceles are incidentally diagnosed on imaging. However, they can become symptomatic when large enough to cause mass effect or when superinfected.[4]

Imaging

Lymphoceles should be readily identifiable on imaging if they measure greater than 1 cm in size. On T2-weighted MR sequences, they exhibit high signal intensity due to their high fluid content, and do not enhance after intravenous contrast administration. Central or peripheral lymphatic vessels may also be connected to lymphoceles.[5]

Management

Small sterile lymphoceles are usually asymptomatic, and typically heal by spontaneous resorption. Large lymphoceles that are symptomatic secondary to mass effect or superinfection may be treated with surgical drainage, marsupialization, aspiration, or percutaneous catheter drainage with sclerotherapy.[4]

Lymphatic Malformations

Pathophysiology

Lymphatic malformations are congenital vascular malformations. Pathogenesis remains elusive, but hypotheses include early failure of mesodermal lymphatic sacs to develop into venolymphatic structures, or disordered growth of lymphatic vessels. Most

From the Duke University Medical Center, Durham, NC.
Address correspondence to Waleska M. Pabon-Ramos, MD, MPH, Duke University Medical Center, DUMC 3808, Room 1502, 2301 Erwin Rd, Duke North, Durham, NC 27710. (e-mail: waly.pr@duke.edu).
The authors report no conflicts of interest.

DOI: 10.1097/RMR.0000000000000130

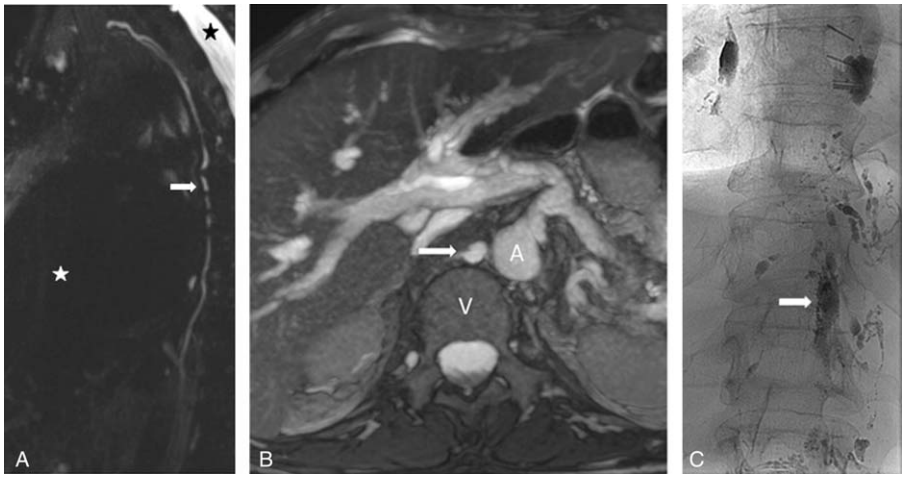

FIGURE 1. MR and fluoroscopic lymphangiography images of the central lymphatic system in 2 different patients demonstrating normal anatomy. A, Sagittal maximum intensity projection (MIP) reconstruction of T2-weighted MRL images in a 33-year-old patient demonstrates normal anatomy of a single thoracic duct (white arrow) as it courses through the thorax. Limited anatomic landmarks are noted on this sequence, as the lungs are of low signal (white star) and spinal fluid is bright on this sequence (black star). B, Axial maximum intensity projection (MIP) reconstruction of balanced gradient images in a 56-year-old patient at the level of T12-L1 demonstrates normal anatomy and location of the retroperitoneal cisterna chyli (white arrow), located immediately anterior to an upper lumbar vertebral body (V) and to the right of the aorta (A). C, Single oblique image of direct intranodal lymphangiogram in a 33-year-old patient seen in image (A) using digital subtraction angiography (DSA) reveals an opacified cisterna chyli (white arrow) at the level of T12-L1. The cisterna chyli is left paramedian in location. The wide cisterna chyli was accessed percutaneously to catheterize and embolize the thoracic duct. Smaller tubular and nodular foci of contrast opacification are compatible with small intrathoracic and intraabdominal lymphatic vessels and lymph nodes, respectively.

frequently diagnosed in children, 90% of lymphatic malformations are identified in patients between birth and 2 years of age.[6] They can be isolated, or part of more extensive syndromes such as Klippel-Trenaunay syndrome. Lymphatic malformations occur within the neck approximately 75% of the time, and less frequently within the axillae and mediastinum.[7] They account for approximately 5% of mediastinal masses.[8] Lymphatic malformations are generally thin-walled, well circumscribed, and insinuate between surrounding anatomic structures. Lymphatic malformations are subdivided into macrocystic, microcystic, or combined macro- and microcystic types, which are differentiated by the size of cystic components. Macrocystic lesions have cystic components greater than 2 cm in diameter.[9] Microcystic lesions have cystic components smaller than 2 cm in diameter, and so appear to be predominantly composed of soft tissue. When a venous component is present, these lesions are considered venolymphatic malformations (Fig. 3).

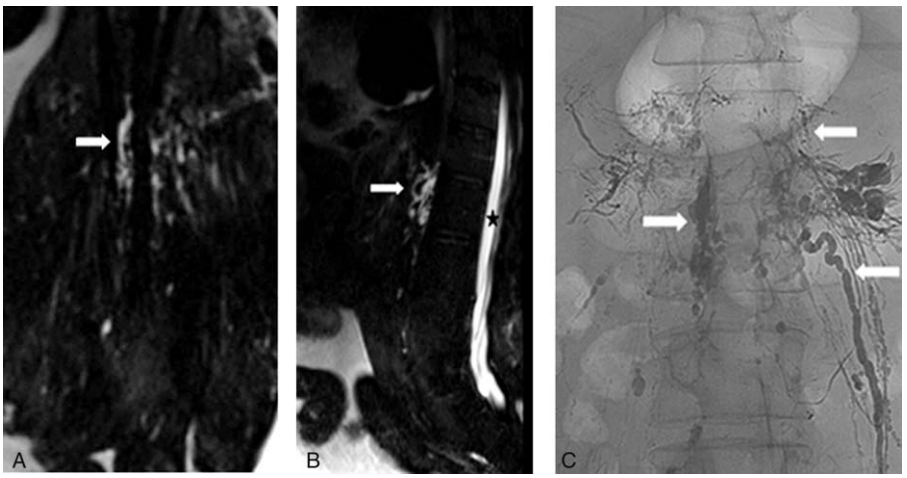

FIGURE 2. MR and fluoroscopic lymphangiography images of the upper abdomen in a 44-year-old patient with chylous ascites demonstrating abnormal ductal anatomy. Coronal MIP T2 weighted MR image (A) and Sagittal MIP T2-weighted MR image (B) at the level of the upper lumbar spine demonstrate nonvisualization of the cisterna chyli. Instead, there are multiple tortuous central retroperitoneal lymphatic vessels (white arrow). (Spinal fluid = black star). C, Frontal image from direct intranodal lymphangiogram using digital subtraction angiography (DSA) of the same patient at the level of the upper lumbar spine reveals numerous opacified retroperitoneal lymphatic vessels (white arrows).

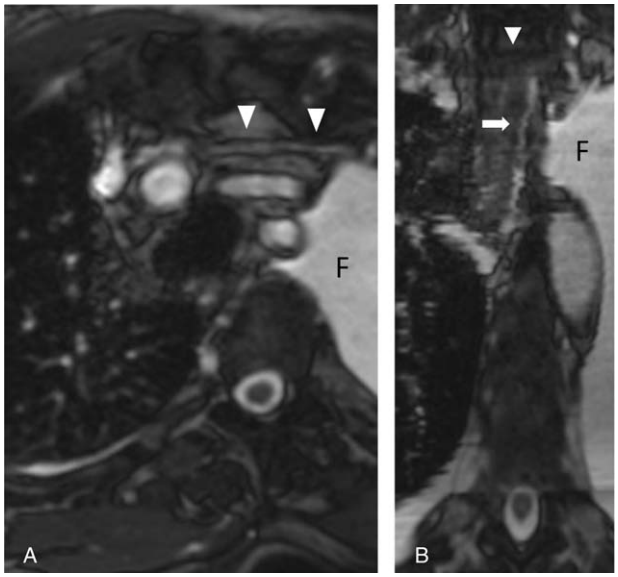

FIGURE 3. MRL images in a 72-year-old patient with chylous pleural effusion demonstrating normal thoracic duct with occluded central vein. A, Single axial oblique balanced gradient image of the chest demonstrates small caliber left brachiocephalic and subclavian vein (white arrowheads) with low signal, consistent with occluded vein. B, Single coronal oblique balanced gradient image of the chest demonstrates a normal thoracic duct (white arrow) coursing from right to left along the upper portion of the thorax. The most cranial portion of the duct is visualized adjacent to the occluded central vein (white arrowhead). (Pleural fluid = F).

Imaging

Macrocystic lymphatic malformations typically exhibit homogeneously low T1 and high T2 signal of the cystic components, and heterogeneous enhancement of septae on contrast-enhanced T1-weighted sequences. The T1 and T2 signal characteristics of the cystic components are variable when septal vessels hemorrhage into the cystic components with consequent thrombus formation, or when the cystic components become superinfected. Findings suggestive of infection include peripheral fat stranding, and robust enhancement of thickened septae. Microcystic lymphatic malformations most frequently appear as predominantly soft tissue masses with small cystic components, and they exhibit low signal intensity on T1-weighted images, high signal intensity on T2-weighted images, and heterogeneous enhancement on postcontrast T1-weighted images. Dynamic contrast enhanced imaging can assist with identification of mixed venolymphatic components, when they are present.

Management

Macrocystic lesions can be treated by percutaneous sclerotherapy with reported response of 91% and complete resolution in 28% in treated patients.[10] Microcystic lesions have traditionally required surgical resection to avoid complications such as superinfection and growth with mass effect. Due to the propensity of these lesions to insinuate into nearby structures, complete resection can be difficult and recurrence is common. However, recent studies show that percutaneous treatment of microcystic lesions with aspiration and doxycycline sclerotherapy resolved 100% of lesions.[11] When lesions are located immediately adjacent to a neurovascular bundle, percutaneous intervention is preferred due to lower risk for injury to the adjacent nerves and vessels as compared with open surgical resection. Identification of a lesion, extent of involvement, description of tissue plane involvement, and relationship to adjacent structures (especially neurovascular bundles) is crucial for the treating physician whether the lesion is to undergo percutaneous or surgical treatment.[12]

Chylothorax

Pathophysiology

Chylothorax is a rare entity that is most commonly acquired. Etiologies include trauma, infection, sarcoidosis, amyloidosis, or malignancy. Approximately 25% of cases result from trauma, either accidental or iatrogenic. Chylothorax is diagnosed clinically, by identifying the typical milky appearance of the pleural effusion. If the pleural fluid is not milky, which is commonly seen after patients are started on a low-fat diet or made NPO, then the chylous nature of the effusion may be established by the presence of triglycerides or chylomicrons in fluid analysis.

Imaging

On MR, chylothorax most commonly manifests as a unilateral pleural effusion. The pleural fluid is often of high T2 signal intensity. Direct communication between the thoracic duct and the chylous pleural fluid generally cannot be seen on noncontrast-enhanced MRL protocols, and requires fluoroscopic lymphangiography or dynamic contrast enhanced MRL with direct intranodal administration of gadolinium into the inguinal nodes.

Management

Conservative therapy for chylothorax includes dietary management, including a low-fat diet, or cessation of oral intake with initiation of total parenteral nutrition, with or without octreotide. This has a reported success rate of 28%. Although surgical thoracic duct ligation is the therapeutic gold standard, it carries morbidity and mortality rates of 38% and 2.1%, respectively.[13] Thoracic duct embolization (TDE), described in 1996 by Cope,[14] is a minimally invasive fluoroscopy-guided procedure that has demonstrated clinical success rates of 72% to 90% in the largest series. Complications from this procedure are generally minor and occur infrequently (rates of 2% to 6%). Complications typically relate to traversal of intra-abdominal organs while accessing the cisterna chyli and asymptomatic pulmonary embolization of lipiodol without long-term sequelae.[15,16]

Plastic Bronchitis

Pathophysiology

Plastic bronchitis is a rare and frequently fatal condition characterized by the development of chylous bronchial casts and consequent airway obstruction. This entity has been described in pediatric patients with congenital heart disease who have undergone the Fontan procedure. Reports of its development note an association with underlying pulmonary, cardiac, or lymphatic disorders, possibly due to incidental lymphatic injury or the development of anomalous lymphatic channels.[17] Plastic bronchitis is diagnosed clinically by the presence of chylous casts upon expectoration or tracheal suction or bronchoscopy.

Imaging

MRL findings suggestive of plastic bronchitis include dilated peritracheal lymphatics that communicate with a patent normal sized thoracic duct.[17]

TABLE 1. Noncontract and Contrast-enhanced Magnetic Resonance Lymphangiography (MRL) Protocols

	Protocol 1: Noncontrast*	Protocol 2: Contrast Enhanced[19]
Contrast	None	Direct intranodal contrast injection into the inguinal lymph nodes (5–10 mL gadolinium/node)
Central duct visualization	Respiratory triggered coronal and sagittal heavily T2-weighted lymphangiography sequence	Breath-hold coronal T1-weighted post-gadolinium administration imaging performed every q1 minute until central lymphatic system is opacified (THRIVE, VIBE, LAVA, Fast FE)
Anatomy of the chest and abdomen	Axial balanced refocused post-excitation gradient sequence (TruFISP, FIESTA, Balanced FFE, True SSFP)	Postcontrast axial short tau inversion recovery sequence (STIR)

*Hurwitz LM, personal communication.

Management

Conservative management with sildenafil and inhaled tPA has been the mainstay of therapy for this entity. Recently, embolization of abnormal thoracic duct branches or the thoracic duct itself has been clinically successful.[18]

MR Technique for Imaging the Central Lymphatic System

Fluoroscopic lymphangiography is considered the gold standard for diagnostic imaging of the central and peripheral lymphatic systems. Fluoroscopic lymphangiography provides high spatial resolution anatomic imaging and allows for physiologic monitoring of flow along the lymphatics. However, fluoroscopic lymphangiography is limited by need for local expertise, direct access of the lymphatic system through pedal lymphatic vessels or inguinal lymph nodes, and radiation exposure while imaging slow lymphatic flow through the lymphatic system. Nuclear scintigraphy has been used as an alternative for invasive lymphangiography but is hampered by low spatial resolution and lack of anatomic landmarks. Multidetector computed tomography has not been used in clinical practice for dedicated lymphatic imaging due to concerns for radiation exposure and its inability to characterize the anatomy and function of the lymphatic system without percutaneous administration of lipiodol. MRI of the lymphatic (MRL) system can depict small and large sized lymphatic ducts using noncontrast and contrast-enhanced protocols (Table 1).[19] The recently published ACR guidelines from 2017 regarding chylothorax treatment assign contrast-enhanced and noncontrast MRL an appropriateness score of 7 (usually appropriate) for chylothorax of nontraumatic or unknown etiology, and a score of 6 (may be appropriate) for chylothorax of traumatic etiology.[20]

MRL examinations can be used to (1) identify and characterize pathologic changes and lesions of the lymphatic system and (2) assess patency and anatomy of the lymphatic and venous systems for pre-intervention planning. For the former, a combination of T1 and T2 imaging with dynamic contrast enhancement can be focused on palpable superficial or mediastinal masses within a targeted anatomic location. For the latter, imaging needs to cover the entire length of the central duct from the level of the cisterna chyli to its termination point at the central veins, which can be accomplished using either noncontrast and contrast sequences or a combination that images the lymphatics and veins.[19]

Normal lymphatic ducts can be challenging to image due to their small size (under 4 mm in width); high spatial resolution imaging using overlapping thin slice acquisition is important for adequate characterization. Cardiac and respiratory motion can lead to obscuration of the small caliber central lymphatic system, and optimization of acquisition techniques to minimize cardiac and respiratory motion artifacts requires use of respiratory gating and fast sequence imaging when possible. Fluid-filled lymphatics can be visualized using high T2-weighted imaging, similar to that which is used for dedicated biliary MRI. For noncontrast MRL, acquisition of a balanced refocused postexcitation gradient MR sequence is very helpful for anatomic correlation. Imaging following thoracic surgery can be optimized with a correlative chest radiograph to note location of surgical clips that produce susceptibility artifact on MR sequences. Direct access of the lymphatic system via inguinal nodes can allow for dynamic assessment of lymphatic flow and communication of lymphatic flow to the abdominal cavity or pleural space (Table 1).

Venous imaging is integral to MRL due to lymphatic outflow to the central veins, the mixed nature of lymphatic-venous disorders, and for pre-procedural planning for TDE. Occlusion of the central veins can lead to lymphatic obstruction (Fig. 4). The central veins should be assessed for patency, areas of stenosis or thrombosis, and location of connection of the lymphatic outflow to the central venous system. Differentiation of venous structures from the lymphatic system should be apparent due to difference in size and course along the thorax, although this can be a challenge with focal venolymphatic malformation or a lymphatic mass with similarly sized veins and lymphatics located in close proximity. The use of intravenous contrast administration and dynamic imaging can help identify the individual lymphatic and venous components.

MR Noncontrast Imaging Procedure

Noncontrast MRL can be performed on 1.5-T or 3-T clinical imaging machines. Patients are imaged in the supine position. ECG leads are placed on the patient's chest for cardiac gating and anterior elements of phased-array coils are then placed over the chest, abdomen, and pelvis. Respiratory gating monitors are utilized for all sequences to reduce respiratory motion artifact.

Anatomic images are acquired using a steady-state balanced gradient series in the axial plane with coverage from the lower neck through the femoral heads using no angulation. Five millimeter slice thickness is used with 40% slice overlap and voxel size $1.2 \times 1.2 \times 1.5\,mm^3$.

Thoracic duct images are obtained using coronal and sagittal heavy T2 3D volume sequence using no angulation. Z-axis coverage from the lower neck through the femoral heads is obtained in 2 stations with at least 20 mm overlap; in the sagittal plane, coverage in the lateral direction extends from midclavicular line to midclavicular line; in the coronal plane, coverage in the anterior-to-posterior direction includes the anterior chest wall through the mid-thoracic vertebral body level. Technical parameters are as follows: phase encoding direction: right-to-left (coronal) and anterior-to-posterior (sagittal); repetition time/echo time: 2000 ms/97 ms; flip angle: 140°;

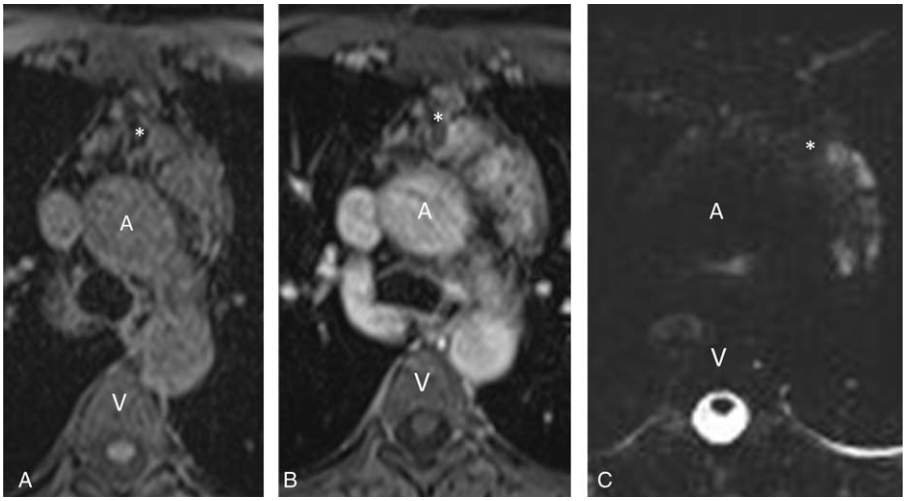

FIGURE 4. Axial MR images in a 33-year-old patient with an anterior mediastinal microcystic venolymphatic malformation. Axial T1-weighted pre (A) and postcontrast (B) MR images demonstrate a mass (∗) in the anterior mediastinum that is isointense to adjacent mediastinal structures and enhances with contrast on delayed phased images. C, T2-weighted MR images demonstrate several small cystic components that do not exceed 2 cm in size. Findings are consistent with microcystic venolymphatic malformation. (A = ascending aorta, V = vertebral body).

slice thickness: 1 mm without overlap; field-of-view: 400 mm; voxel size: $0.9 \times 0.9 \times 1.0\,mm^3$; turbo factor: 270; bandwidth: 501 Hz.

MR Dynamic Contrast Enhanced Imaging Procedure:

Dynamic contrast enhanced MRL was recently described by Krishnamurthy et al,[19] and is performed by direct intranodal injection of dilute gadolinium (1 : 1 dilution with normal saline) into the inguinal lymph nodes. Lymph node access is obtained by the ultrasound-guided placement of a 20 to 23-gauge spinal needle or angiographic catheter into the inguinal nodes, after which correct positioning can be confirmed by saline injection.

Following catheter placement, initial survey images are used to confirm positioning and coverage, which should extend from the middle of the neck to the inguinal region, or, in larger patients, from the middle of neck through the lower abdomen. Noncontrast and contrast-enhanced fat suppressed images are obtained using a breath-hold 3-dimensional spoiled gradient echo sequence with an acquired voxel size: $1–1.3 \times 1–1.3 \times 2–2.6\,mm^3$; reconstructed voxel size: $0.65–1 \times 0.65–1 \times 1–1.3\,mm^3$.

Five to ten milliliters of dilute gadolinium is then slowly infused (approximately 1 mL/3 minutes).[21] During contrast administration, imaging is obtained every 2 minutes using a spoiled gradient echo sequence until contrast material is seen in the retroperitoneal lymphatics. Subsequent imaging every 30 seconds to 1 minute occurs with filling of the central duct. Following lymphangiography, anatomic imaging can be obtained with a short tau inversion recovery (STIR) sequence.[19]

Image Processing

Anatomic and MRL-specific sequences should be viewed simultaneously on a PACS workstation and dedicated 3D post-processing platform to relate anatomic structures to the lymphatic system and venous system. T2-weighted sagittal and coronal images provide the most coverage for the least amount of time when compared with axial images, and can be reformatted into an axial plane for direct correlation with the anatomic images. Interactive off-axis assessment using maximal intensity projection can be very helpful for visualization of the thoracic duct and its connection to the central venous system. Selective editing of the volumetric datasets with removal of the high signal spinal fluid and pleural fluid will allow for improved visualization of the central duct on post-processing software platforms for 3D volume rendered images.

Interpretation and Reporting

Diagnostic MRL studies for lymphatic mass characterization should include characterization of the components of a mass, and whether a lesion is purely lymphatic, mixed lymphatic, venous, or arterial. Extent of mass, connection to the central lymphatic system, and involvement of adjacent muscular, vascular, and neurologic structures should be described to the extent possible.

Most referring physicians recognize limitations of MR in the delineation of extensive tiny ducts. Delineation of landmarks for use with intraoperative or percutaneous intervention is best provided by correlation with bony structures or surgical hardware, if present. Correlative radiographs or CT at the time of MRI can be very beneficial for correlation and next step procedures.

Role of MRL in Preprocedural Planning for Thoracic Lymphatic Disorders

MRL can provide guidance for medical, surgical, and minimally invasive procedures. Open surgical approaches require an understanding of the extent of lesions and relationship to adjacent structures. Lymphatic malformations with proximity to or involving critical neurovascular structures may be better treated with minimally invasive procedures. Identification of the location of thoracic duct disruption is critical for successful surgical thoracic duct ligation.

Anatomic evaluation of the thoracic duct by MRL is especially useful for planning TDE.[16,17] TDE can be performed by antegrade catheterization of the thoracic duct by accessing the cisterna chyli percutaneously, or by retrograde catheterization of the thoracic duct through its central venous outflow. Anatomic evaluation on MRL includes localization of the cisterna chyli, venous thoracic duct outflow, description of variant central lymphatic anatomy, and evaluation

of the central veins of the upper torso. The absence of a cisterna chyli or variant location is important for planning percutaneous access, and when the cisterna chyli is absent, MRL may show if there are prominent retroperitoneal lymphatic trunks that may serve as alternate targets for percutaneous access. For transvenous retrograde lymphangiography, which may be performed in patients with intracardiac shunts that place them at risk of stroke from lipiodol embolization or in patients who lack a cisterna chyli, MRL reveals the location of the outflow of the thoracic duct. This increases the likelihood of successful retrograde catheterization of the thoracic duct.

CONCLUSION

With improvements in image quality owing to advances in MRI hardware and software, MRL has expanded in use to address the increasing need for characterization of lymphatic masses, pre-procedural planning, and definitive lymphatic interventions. Multidisciplinary groups of radiologist, interventionalists, and surgeons working to optimize imaging and treatment planning will advance the applications of MR to diagnosis and management of lymphatic disorders and improve patient care.

REFERENCES

1. De-xin Y, Xiang-xing M, Xiao-ming Z, et al. Morphological features and clinical feasibility of thoracic duct: detection with nonenhanced magnetic resonance imaging at 3.0 T. J Magn Reson Imaging 2010;32:94–100.
2. Geschwind JFH, Dake MD. Abrams' Angiography, 3rd ed. Philadelphia, PA: Lippincott Williams and Wilkins; 2014.
3. Pinto PS, Sirlin CB, Andrade-Barreto OA, et al. Cisterna Chyli at routine abdominal MR imaging: a normal anatomic structure in the retrocrural space. *RadioGraphics*. 2004;24:809–817.
4. Ge W, Yu D-C, Chen J, et al. Lymphocele: a clinical analysis of 19 cases. *Int J Clin Exp Med*. 2015;8:7342–7350.
5. Hamilton BE, Nesbit GM, Gross N, et al. Characteristic imaging findings in lymphoceles of the head and neck. *AJR Am J Roentgenol*. 2011;197:1431–1435.
6. Shah GH, Deshpande MD. Lymphatic malformation in adult patient: a rare case. *J Maxillofac Oral Surg*. 2010;9:284–288.
7. Breugem CC, Van der horst CM, Hennekam RC. Progress toward understanding vascular malformations. *Plast Reconstr Surg*. 2001;107:1509–1523.
8. Park JG, Aubry MC, Godfrey JA, et al. Mediastinal lymphangioma: Mayo Clinic experience of 25 cases. *Mayo Clin Proc*. 2006;81:1197–1203.
9. Perkins JA, Manning SC, Tempero RM, et al. Lymphatic malformations: review of current treatment. *Otolaryngol Head Neck Surg*. 2010;142:795–803.803.e1.
10. Mohan AT, Adams S, Adams K, et al. Intralesional bleomycin injection in management of low flow vascular malformations in children. *J Plast Surg Hand Surg*. 2015;49:116–120.
11. Shiels WE, Kang DR, Murakami JW, et al. Percutaneous treatment of lymphatic malformations. *Otolaryngol Head Neck Surg*. 2009;141:219–224.
12. Khunger N. Lymphatic malformations: current status. *J Cutan Aesthet Surg*. 2010;3:137–138.
13. Cerfolio RJ, Allen MS, Deschamps C, et al. Postoperative chylothorax. *J Thorac Cardiovasc Surg*. 1996;112:1361–1366.
14. Cope C. Percutaneous transabdominal embolization of thoracic duct lacerations in animals. *J Vasc Interv Radiol*. 1996;7:725–731.
15. Itkin M, Kucharczuk JC, Kwak A, et al. Nonoperative thoracic duct embolization for traumatic thoracic duct leak: experience in 109 patients. *J Thorac Cardiovasc Surg*. 2010;139:584–589.
16. Pamarthi V, Stecker MS, Schenker MP, et al. Thoracic duct embolization and disruption for treatment of chylous effusions: experience with 105 patients. *J Vasc Interv Radiol*. 2014;25:1398–1404.
17. Itkin MG, Mccormack FX, Dori Y. Diagnosis and treatment of lymphatic plastic bronchitis in adults using advanced lymphatic imaging and percutaneous embolization. *Ann Am Thorac Soc*. 2016;13:1689–1696.
18. Dori Y, Keller MS, Rychik J, et al. Successful treatment of plastic bronchitis by selective lymphatic embolization in a Fontan patient. *Pediatrics*. 2014;134:e590–e595.
19. Krishnamurthy R, Hernandez A, Kavuk S, et al. Imaging the central conducting lymphatics: initial experience with dynamic MR lymphangiography. *Radiology*. 2015;274:871–878.
20. Majdalany BS, Murrey DA, Kapoor BS, et al. ACR Appropriateness Criteria: Chylothorax Treatment Planning. Available at: https://www.acr.org/Quality-Safety/Appropriateness-Criteria/New-and-Revised. Accessed October 1, 2017.
21. Kariya S, Komemushi A, Nakatani M, et al. Intranodal lymphangiogram: technical aspects and findings. *Cardiovasc Intervent Radiol*. 2014;37:1606–1610.